European Radiology (2019) 29:6119–6128
https://doi.org/10.1007/s00330-019-06221-9

CARDIAC

Relevance of anatomical, plaque, and hemodynamic characteristics of non-obstructive coronary lesions in the prediction of risk for acute coronary syndrome

Jiesuck Park[1] · Joo Myung Lee[2] · Bon-Kwon Koo[1,3] · Gilwoo Choi[4] · Doyeon Hwang[1] · Tae-Min Rhee[1] · Seokhun Yang[1] · Jonghanne Park[1] · Jinlong Zhang[1] · Kyung-Jin Kim[1] · Yaliang Tong[5] · Joon-Hyung Doh[6] · Chang-Wook Nam[7] · Eun-Seok Shin[8] · Young-Seok Cho[9] · Eun Ju Chun[10] · Jin-Ho Choi[2] · Bjarne L. Norgaard[11] · Evald H. Christiansen[11] · Koen Nieman[12,13] · Hiromasa Otake[14] · Martin Penicka[15] · Bernard de Bruyne[15] · Takashi Kubo[16] · Takashi Akasaka[16] · Jagat Narula[17] · Pamela S. Douglas[18] · Charles A. Taylor[4,19]

Received: 8 February 2019 / Revised: 31 March 2019 / Accepted: 3 April 2019 / Published online: 25 April 2019

Abstract

Objectives We explored the anatomical, plaque, and hemodynamic characteristics of high-risk non-obstructive coronary lesions that caused acute coronary syndrome (ACS).

Methods From the EMERALD study which included ACS patients with available coronary CT angiography (CCTA) before the ACS, non-obstructive lesions (percent diameter stenosis < 50%) were selected. CCTA images were analyzed for lesion characteristics by independent CCTA and computational fluid dynamics core laboratories. The relative importance of each characteristic was assessed by information gain.

Results Of the 132 lesions, 24 were the culprit for ACS. The culprit lesions showed a larger change in FFR_{CT} across the lesion (ΔFFR_{CT}) than non-culprit lesions (0.08 ± 0.07 vs 0.05 ± 0.05, $p = 0.012$). ΔFFR_{CT} showed the highest information gain (0.051, 95% confidence interval [CI] 0.050–0.052), followed by low-attenuation plaque (0.028, 95% CI 0.027–0.029) and plaque volume (0.023, 95% CI 0.022–0.024). Lesions with higher ΔFFR_{CT} or low-attenuation plaque showed an increased risk of ACS (hazard ratio [HR] 3.25, 95% CI 1.31–8.04, $p = 0.010$ for ΔFFR_{CT}; HR 2.60, 95% CI 1.36–4.95, $p = 0.004$ for low-attenuation plaque). The prediction model including ΔFFR_{CT}, low-attenuation plaque and plaque volume showed the highest ability in ACS prediction (AUC 0.725, 95% CI 0.724–0.727).

Conclusion Non-obstructive lesions with higher ΔFFR_{CT} or low-attenuation plaque showed a higher risk of ACS. The integration of anatomical, plaque, and hemodynamic characteristics can improve the noninvasive prediction of ACS risk in non-obstructive lesions.

Key Points

- *Change in FFR_{CT} across the lesion (ΔFFR_{CT}) was the most important predictor of ACS risk in non-obstructive lesions.*
- *Non-obstructive lesions with higher ΔFFR_{CT} or low-attenuation plaque were associated with a higher risk of ACS.*
- *The integration of anatomical, plaque, and hemodynamic characteristics can improve the noninvasive prediction of ACS risk.*

Keywords Plaque, atherosclerotic · Acute coronary syndrome · Coronary stenosis · Hemodynamics · Computed tomography angiography

Jiesuck Park and Joo Myung Lee contributed equally to this work.

Electronic supplementary material The online version of this article (https://doi.org/10.1007/s00330-019-06221-9) contains supplementary material, which is available to authorized users.

✉ Bon-Kwon Koo
bkkoo@snu.ac.kr

Extended author information available on the last page of the article

Abbreviations

%DS	Percent diameter stenosis
ACS	Acute coronary syndrome
AUC	Area under the curve
CCTA	Coronary computed tomography angiography
CFD	Computational fluid dynamics
FFR_{CT}	Coronary CT angiography-derived fractional flow reserve

MI	Myocardial infarction
SCD	Sudden cardiac death
ΔFFR_{CT}	Delta FFR_{CT}

Introduction

The primary goal of coronary revascularization is to identify and treat advanced coronary artery disease (CAD) with obstructive stenoses. Introduction of coronary computed tomography angiography (CCTA) has exerted a considerable impact on the diagnosis of CAD by allowing noninvasive assessment of anatomical severity and plaque characteristics of the coronary lesions [1–4]. Additionally, noninvasive or invasive hemodynamic stress tests have enabled to detect the ischemia-causing stenosis [5]. Of the various physiologic indices, fractional flow reserve (FFR) has been considered as a gold standard to identify ischemia-causing coronary stenoses [5]. A recent advance in computational fluid dynamics (CFD) has made it possible to calculate and visualize blood flow and pressure fields along the coronary vessels [6]. Combining the CFD technique with the anatomical information of CCTA, it is possible to calculate FFR (CCTA-derived fractional flow reserve [FFR_{CT}]) without additional invasive procedures or hyperemic agents [7–9]. Recently, the EMERALD (Exploring the Mechanism of the plaque Rupture in Acute coronary syndrome using coronary CT Angiography and computationaL fluid Dynamics) study demonstrated improvement in prediction of acute coronary syndrome (ACS) by adding noninvasive hemodynamic parameters over anatomical and plaque characteristics using CCTA and CFD [10].

Meanwhile, a substantial proportion of patients with sudden cardiac death (SCD) do not have known obstructive coronary disease [11, 12]. Therefore, identification of high-risk plaque for subsequent adverse cardiovascular events is essential, not only for patients with obstructive or severe coronary stenoses but also for those with non-obstructive coronary stenoses. The current study aimed to investigate the anatomical, plaque, and hemodynamic characteristics of high-risk non-obstructive coronary lesions that caused acute coronary syndrome.

Materials and methods

Study population

The study population was derived from the EMERALD study [10]. In brief, patients who experienced a documented ACS event (acute myocardial infarction or unstable angina with objective evidence of plaque rupture) and had undergone CCTA from 1 month to 2 years before the ACS event were enrolled. All patients underwent invasive coronary angiography at the time of the ACS event. Patients with ACS related to in-stent restenosis, secondary MI due to other general medical conditions, previous history of coronary artery bypass graft surgery or poor image quality of CCTA for CFD analysis were excluded. All angiograms were reviewed at a core laboratory in Seoul National University Hospital, and the culprit lesions were determined in a blinded fashion. The current study selected non-obstructive lesions with percent diameter stenosis (%DS) < 50% assessed by CCTA. The detailed study flow is summarized in Supplementary Fig. 1. Among 59 patients, CCTA images were acquired using Siemens scanners (Somatom Definition or Somatom Definition Flash) in 47 patients (98 lesions, 79.7%) and Philips scanners (Philips Brilliance 64 or Brilliance iCT) in 12 patients (34 lesions, 20.3%). The study protocol was approved by the institutional review board of each site and was conducted following the Declaration of Helsinki (ClinicalTrials.gov Identifier: NCT02374775).

CCTA analysis for plaque characteristics

CCTA images were screened and analyzed for anatomical and plaque characteristics at a core laboratory in Seoul National University Bundang Hospital by an independent observer (EJC, MD, PhD, 11 years of experience in cardiac imaging) blinded to both the clinical data and CFD results. For anatomical characteristics, %DS, minimal luminal diameter, lesion length, plaque volume, and plaque burden were measured. The plaque burden was defined as [plaque volume/vessel volume] × 100 at a target lesion. The lesions with %DS > 30% based on CCTA assessment were further evaluated for plaque characteristics. The presence of low-attenuation plaque (average density ≤ 30 Hounsfield unit [HU]) and positive remodeling (remodeling index ≥ 1.1) was assessed as adverse plaque characteristics in the same manner as previous studies [13, 14]. Briefly, the plaque density was measured semi-automatically by dedicated cardiac workstation (Intellispace Portal, Philips Healthcare). The average plaque density was defined by the mean value of HU measured at least five randomly selected points in the lesion as a region of interest. The remodeling index was calculated as the vessel diameter at the site of maximal stenosis divided by the reference diameter.

CCTA image analysis for hemodynamic parameters

All CFD analyses for hemodynamic parameters were performed in a blinded fashion using the same procedure performed during FFR_{CT} computation at a core laboratory in HeartFlow, Inc. [7, 8, 15]. The patient-specific anatomic model of coronary arteries was reconstructed from CCTA images with segmentation of lumen boundary. Blood flow, pressure,

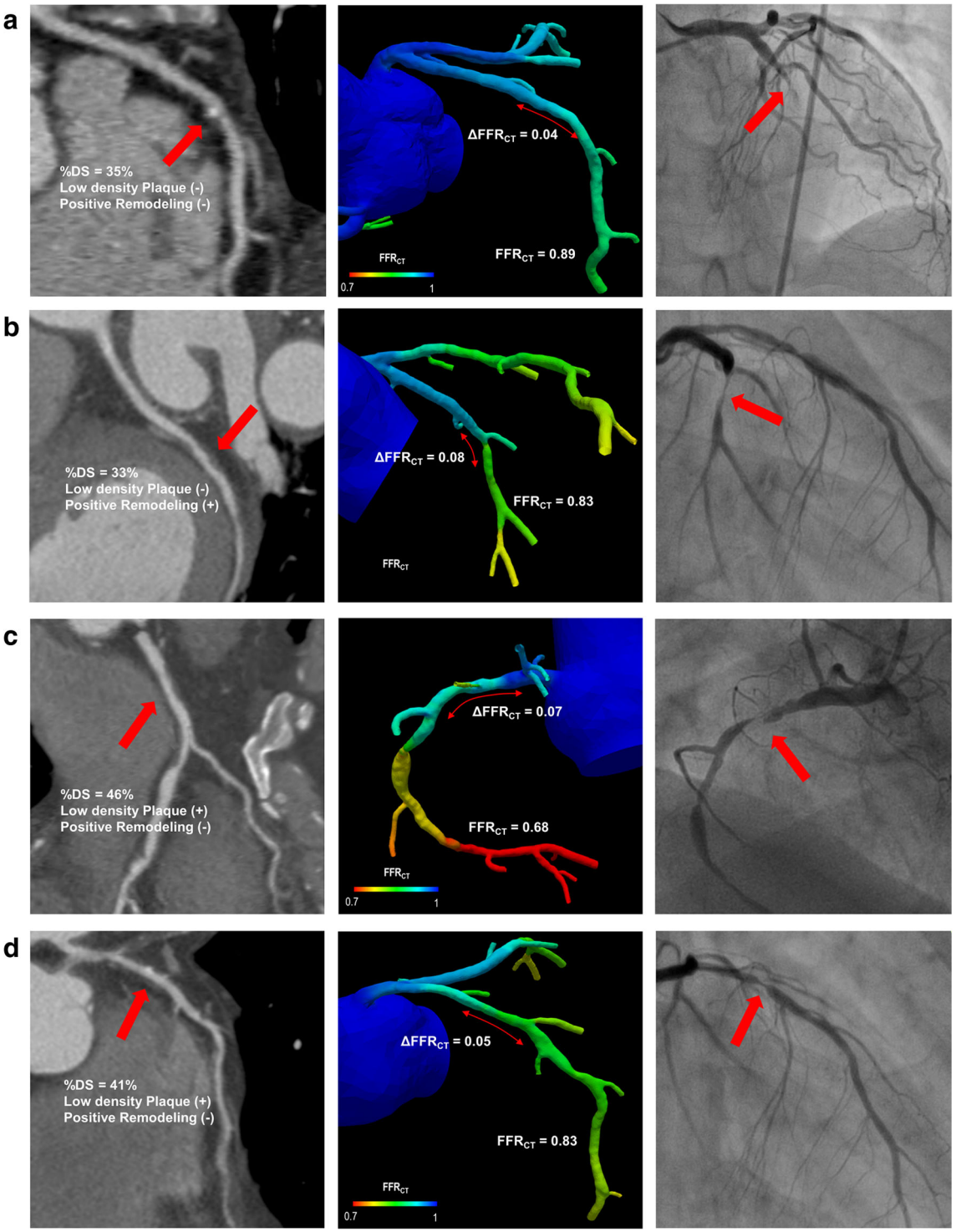

Fig. 1 Representative cases of non-obstructive lesions causing acute coronary syndrome. Four cases of non-obstructive lesions causing acute coronary syndrome are presented in Fig. 1. Case A: The coronary CT angiography (CCTA) showed that the lesion in mid left anterior descending coronary artery (LAD) had 35% diameter stenosis (%DS) and did not have low-attenuation plaque nor positive remodeling. Per-vessel FFR_{CT} was 0.89 and ΔFFR_{CT} was 0.04. After 514 days from CCTA, the patient presented with acute myocardial infarction with obstruction of mid-LAD. Case B: The lesion in distal left circumflex artery (LCX) had 33% DS with positive remodeling. Per-vessel FFR_{CT} was 0.83 and ΔFFR_{CT} was 0.08. After 269 days from CCTA, the patient presented with acute myocardial infarction with near total obstruction of distal LCX. Case C: The lesion in right coronary artery (RCA) had 46% DS and low-attenuation plaque. Per-vessel FFR_{CT} was 0.68 and ΔFFR_{CT} was 0.07. After 161 days from CCTA, the patient presented with acute myocardial infarction with near total occlusion and plaque rupture of proximal RCA. Case D: CCTA shows the lesion in mid-LAD with 41% DS and low-attenuation plaque. Per-vessel FFR_{CT} was 0.83 and ΔFFR_{CT} was 0.05. After 269 days from CCTA, the patient presented with acute myocardial infarction with near total obstruction of mid-LAD. %DS, percent diameter stenosis; FFR_{CT}, coronary CT angiography-derived fractional flow reserve; ΔFFR_{CT}, change in FFR_{CT} across the lesion

and hyperemic response along the coronary trees were computed using CFD technique by solving the Navier-Stokes equations [7, 8]. For the current study, two clinically applicable hemodynamic parameters, per-vessel FFR derived from CCTA (FFR_{CT}) and change in FFR_{CT} across the lesion (ΔFFR_{CT}), were used as noninvasive hemodynamic parameters (Fig. 1). FFR_{CT} was defined as the ratio of mean pressure in downstream coronary vessels (Pd) to that of the aorta (Pa). ΔFFR_{CT} was derived by calculating the difference between the proximal and distal FFR_{CT} (ΔFFR_{CT} = proximal FFR_{CT} − distal FFR_{CT}).

Statistical analysis

Characteristics of the culprit and non-culprit lesions were analyzed on a per-lesion basis. Continuous variables were presented either as means with standard deviations or medians with interquartile ranges (IQR). Categorical variables were presented as numbers and relative frequencies (percentages). For the per-lesion-based comparison of anatomical, plaque, and hemodynamic characteristics between culprit and non-culprit lesions, the generalized estimating equation was used to adjust for intra-subject variability. Correlation analysis was used to assess the degree of relationship between FFR_{CT} or ΔFFR_{CT} and %DS.

The information gain of each variable with a 10,000-permutation resampling method was calculated to compare the relative significance of the lesion characteristics on subsequent ACS events. The information gain represents the contribution of a predictor for the event of interest, which is calculated by the differences in entropy before and after classifying the data based on the predictor [16]. The higher information gain indicates that the predictor is more important for explaining the event, which for the current study was identifying the culprit lesion(s). In addition, to evaluate the impact of each lesion characteristic on subsequent ACS risk, the lesions were classified by the presence of adverse lesion characteristics and compared using marginal Cox regression analysis. Continuous values of anatomical and hemodynamic parameters were converted to binary variables by using mean or median values for defining the presence of adverse anatomical (%DS, 40%; minimal luminal diameter, 2.2 mm; lesions length, 17.0 mm; plaque volume, 48.1 mm^3; plaque burden, 44.8%) or hemodynamic (FFR_{CT}, 0.84; ΔFFR_{CT}, 0.04) characteristics.

Prediction models for subsequent ACS events were constructed by individual or multiple combinations of the lesion characteristics, and the performance of models was compared using area under the curve (AUC) of the receiver operator characteristics with 10,000-permutation resampling method.

All probability values were two-sided, and p values < 0.05 were considered statistically significant. The statistical package SPSS, version 18.0 (SPSS Inc.), and R, version 3.4.3 (R Development Core Team), were used for statistical analyses.

Results

Baseline characteristics of patients

A total of 132 non-obstructive lesions of 59 patients were selected from the original EMERALD study population. Table 1 presents patient characteristics. The median interval between CCTA and ACS event was 342 days (IQR 167–545 and range 54–703) and 94.9% of patients presented with acute MI.

Comparison of lesion characteristics between culprit and non-culprit lesions

Table 2 shows the anatomical, plaque, and hemodynamic characteristics of the culprit and non-culprit lesions. There were no significant differences in anatomical characteristics between culprit and non-culprit lesions. The prevalence of low-attenuation plaque was higher in culprit lesions without statistical significance (41.7% vs 24.1%, $p = 0.173$). As for hemodynamic characteristics, ΔFFR_{CT}

Table 1 Baseline characteristics of the study patients and lesions

Patients ($N = 59$)	
Age (years)	70.3 ± 12.7
Male	43 (72.9)
Median interval between CCTA and acute coronary syndrome (days)	342.0 (167.0–545.0)
Cardiovascular risk factors	
Hypertension	37 (62.7)
Diabetes mellitus	31 (52.5)
Hypercholesterolemia	27 (45.8)
Current smoker	19 (32.2)
Ejection fraction (%)	58.0 (42.7–63.0)
Clinical presentation	
Myocardial infarction	56 (94.9)
NSTEMI	34 (57.6)
STEMI	22 (37.3)
Unstable angina	3 (5.1)

Values given as mean ± standard deviation, median (interquartile range, 25th and 75th percentiles), or number (percentage), unless otherwise indicated.

CCTA, coronary computed tomography angiography; *NSTEMI*, non-ST-segment elevation myocardial infarction; *STEMI*, ST-segment elevation myocardial infarction

Table 2 Comparison of lesion characteristics between culprit and non-culprit lesions

	All lesions ($N = 132$)	Culprit ($N = 24$)	Non-culprit ($N = 108$)	p value
Anatomical characteristics				
% Diameter stenosis	36.9 ± 9.4	39.7 ± 6.5	36.3 ± 9.9	0.193
Minimal luminal diameter (mm)	2.3 ± 0.6	2.3 ± 0.5	2.3 ± 0.6	0.605
Lesion length (mm)	17.0 ± 7.0	17.8 ± 9.7	16.9 ± 6.3	0.575
Plaque volume (mm^3)	68.7 ± 57.1	71.9 ± 44.7	67.9 ± 59.8	0.211
Plaque burden (%)	44.9 ± 11.7	44.5 ± 11.1	45.0 ± 11.8	0.856
Lesion location				0.579
Left main to LAD	47 (35.6)	36 (33.3)	11 (45.8)	
Left circumflex artery	27 (20.5)	24 (22.2)	3 (12.5)	
Right coronary artery	58 (43.9)	48 (44.5)	10 (41.7)	
Proximal lesion	55 (41.7)	9 (37.5)	46 (42.6)	0.819
Plaque characteristics				
Low-attenuation plaque	36 (27.3)	10 (41.7%)	26 (24.1%)	0.173
Positive remodeling	14 (10.6)	3 (12.5%)	11 (10.2%)	0.682
Hemodynamic characteristics				
FFR_{CT}	0.80 ± 0.13	0.81 ± 0.10	0.80 ± 0.13	0.730
ΔFFR_{CT}	0.05 ± 0.05	0.08 ± 0.07	0.05 ± 0.05	0.012

Values given as mean ± standard deviation, or number (percentage), unless otherwise indicated

FFR_{CT}, coronary CT angiography-derived fractional flow reserve; *ΔFFR_{CT}*, delta FFR_{CT}; *LAD*, left anterior descending coronary artery

was higher in culprit lesions than in non-culprit lesions (0.08 ± 0.07 vs 0.05 ± 0.05, $p = 0.012$). However, there was no difference in FFR_{CT} between culprit and non-culprit lesions (0.81 ± 0.10 vs 0.80 ± 0.13, $p = 0.730$). ΔFFR_{CT} showed mild correlation with %DS ($r = 0.195$, $p = 0.025$); however, there was no significant correlation between FFR_{CT} and %DS ($r = -0.097$, $p = 0.270$).

Relative importance and prognostic significance of lesion characteristic

Among the nine lesion characteristics, ΔFFR_{CT} showed the highest information gain (0.051, 95% confidence interval [CI] 0.050–0.052) followed by low-attenuation plaque (0.028, 95% CI 0.027–0.029) and plaque volume (0.023, 95% CI

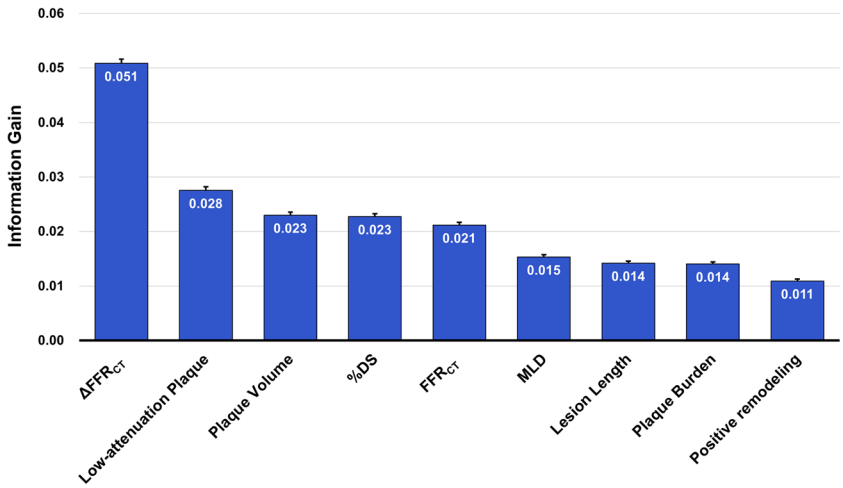

Fig. 2 Importance of individual lesion characteristic assessed by information gain. The figure shows the importance of individual lesion characteristic assessed by information gain using a 10,000-permutation resampling method. ΔFFR_{CT} showed the highest information gain (0.051, 95% CI 0.050–0.052), followed by low-attenuation plaque, plaque volume, and percent diameter stenosis (%DS). %DS, percent diameter stenosis; FFR_{CT}, coronary CT angiography-derived fractional flow reserve; ΔFFR_{CT}, change in FFR_{CT} across the lesion; MLD, minimal luminal diameter

Table 3 Estimated risk for the culprit of acute coronary syndrome according to lesion characteristics

Lesion characteristics	HR	95% CI	*p* value
Anatomical characteristics			
% Diameter stenosis	1.54	0.78–3.02	0.214
Minimal luminal diameter	0.95	0.43–2.11	0.897
Lesion length	1.02	0.45–2.13	0.966
Plaque volume	1.25	0.50–3.12	0.639
Plaque burden	1.15	0.38–2.00	0.749
Plaque characteristics			
Low-attenuation plaque	2.60	1.36–4.95	0.004
Positive remodeling	1.15	0.33–4.03	0.831
Hemodynamic characteristics			
FFR_{CT}	0.54	0.27–1.09	0.101
ΔFFR_{CT}	3.25	1.31–8.04	0.010

FFR_{CT}, coronary CT angiography-derived fractional flow reserve; *ΔFFR_{CT}*, delta FFR_{CT}

0.022–0.024) (Fig. 2). Lesions with higher ΔFFR_{CT} and presence of low-attenuation plaque were associated with a higher risk for the culprit of subsequent ACS (hazard ratio [HR] 3.25, 95% CI 1.31–8.04, $p = 0.010$ and HR 2.60, 95% CI 1.36–4.95, $p = 0.004$ for ΔFFR_{CT} and low-attenuation plaque, respectively) (Table 3 and Fig. 3).

Prediction models for ACS risk among non-obstructive lesion

Table 4 and Fig. 4 present the performance of prediction models for ACS risk. Among the anatomical, plaque, and hemodynamic characteristics, plaque volume (AUC 0.590, 95% CI 0.589–0.591), low-attenuation plaque (AUC 0.590, 95% CI 0.589–0.592), and ΔFFR_{CT} (AUC 0.654, 95% CI 0.652–0.655) showed the highest performance in each category of lesion characteristics, respectively. In multiple combinations, models with ΔFFR_{CT} and either plaque volume (AUC 0.691, 95% CI 0.689–0.692) or low-attenuation plaque (AUC 0.703, 95% CI 0.701–0.705) showed significantly higher performance than the model with plaque volume and low-attenuation plaque (AUC 0.644, 95% CI 0.643–0.646) (p for both < 0.001). The model with ΔFFR_{CT}, low-attenuation plaque, and plaque volume showed the best performance (AUC 0.725, 95% CI 0.724–0.727) among the models.

Discussion

The current study explored the anatomical, plaque, and hemodynamic characteristics of high-risk non-obstructive coronary lesions associated with ACS assessed by noninvasive CCTA and CFD. The main findings of our study are as follows: (1) the culprit lesions showed a higher change in FFR_{CT} across the lesion (ΔFFR_{CT}) than non-culprit lesions. However, there was no difference in FFR_{CT} between the two groups; (2) from information gain analysis, ΔFFR_{CT} was the most important factor associated with ACS event followed by low-attenuation plaque and plaque volume; and (3) the prediction model including ΔFFR_{CT}, low-attenuation plaque, and plaque volume demonstrated the highest predictive ability for ACS event.

Importance of identifying high-risk non-obstructive lesion

Identification of high-risk lesions for subsequent ACS event is important in the management of patients with coronary artery disease. Therefore, invasively or noninvasively detected adverse anatomical and plaque characteristics have been used as indicators of the high-risk plaque [17]. In studies with non-obstructive lesions, Kristensen et al reported that the total amount of non-calcified plaque was a predictor for future

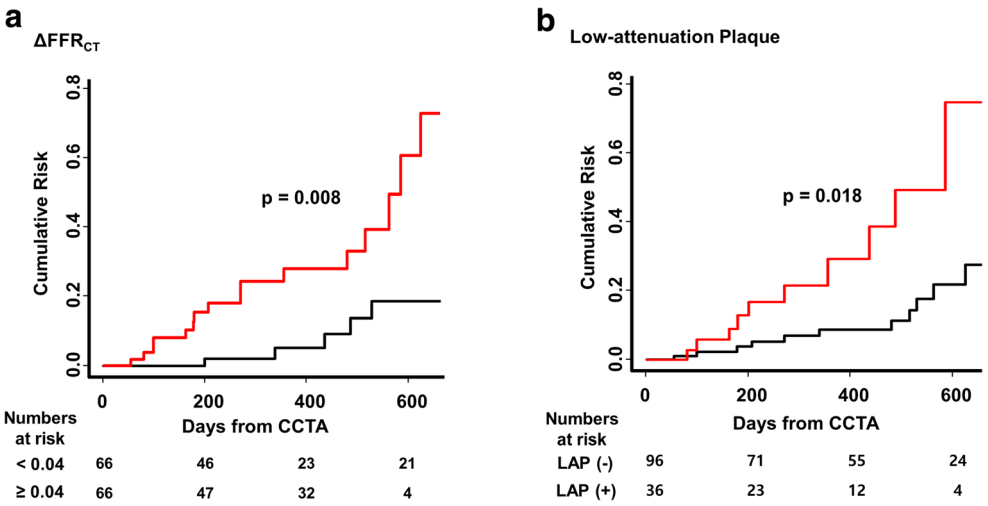

Fig. 3 Cumulative risk for the culprit of future ACS according to lesion characteristics. Lesions with high ΔFFR_{CT} (**a**) or low-attenuation plaque (**b**) showed significantly higher risk for the culprit lesions in future ACS event compared with those with lower ΔFFR_{CT} or absence of low-attenuation plaque, respectively. CCTA, coronary CT angiography; ΔFFR_{CT}, change in FFR_{CT} across the lesion; LAP, low-attenuation plaque

Table 4 Comparison of AUC values in prediction of risk for the culprit of acute coronary syndrome

Lesion characteristics	AUC	95% CI
Anatomical characteristics		
% Diameter stenosis	0.582	0.581–0.583
Lesion length	0.570	0.569–0.571
Plaque volume	0.590	0.589–0.591
Plaque characteristics		
Positive remodeling	0.545	0.544–0.546
Low-attenuation plaque	0.590	0.589–0.592
Hemodynamic characteristics		
FFR_{CT}	0.585	0.584–0.586
ΔFFR_{CT}	0.654	0.652–0.655

AUC, area under the curve; *CI*, confidence interval; FFR_{CT}, coronary CT angiography-derived fractional flow reserve; ΔFFR_{CT}, delta FFR_{CT}

acute coronary events [18] and Ferraro et al showed that non-obstructive lesions with high-risk plaque characteristics had a comparable risk of ACS to obstructive lesions without high-risk plaque characteristics [19]. In addition to anatomical and plaque characteristics, recent studies showed the importance of hemodynamic parameters in the progression and vulnerable transformation of coronary plaque [10, 20, 21]. Our study investigated the absolute and relative significance of anatomical, plaque, and hemodynamic characteristics and found that ΔFFR_{CT}, low-attenuation plaque, and plaque volume were the highest relevant factors in each category for the prediction of culprit lesions for the ACS event.

Prognostic importance of ΔFFR_{CT} among non-obstructive lesions

In our study, ΔFFR_{CT} was the most important factor associated with ACS event among the various lesion characteristics. ΔFFR_{CT} showed the highest information gain and the lesions with high ΔFFR_{CT} were associated with significantly higher risk of culprit for subsequent ACS (HR 3.25, 95% CI 1.31–8.04, $p = 0.010$). It is interesting to note that there was no difference in FFR_{CT} between the culprit and non-culprit lesions. Lee et al investigated the prognostic significance of invasively measured FFR among non-obstructive lesions and found that the risk of a clinical event was higher in the low FFR group than in the high FFR group [22]. However, the association of ΔFFR_{CT} with ACS risk was not investigated in that study. In our study, the correlation between %DS and ΔFFR_{CT} was significant whereas no significant relationship was found between %DS and FFR_{CT}. Previous studies showed that the external plaque stress increases as the pressure gradient across the lesion increases [21, 23–25]. Taken together, ΔFFR_{CT} may demonstrate a more significant effect on ACS event than per-vessel FFR in the non-obstructive lesion. However, the relative importance of per-vessel FFR and ΔFFR_{CT} needs further investigation.

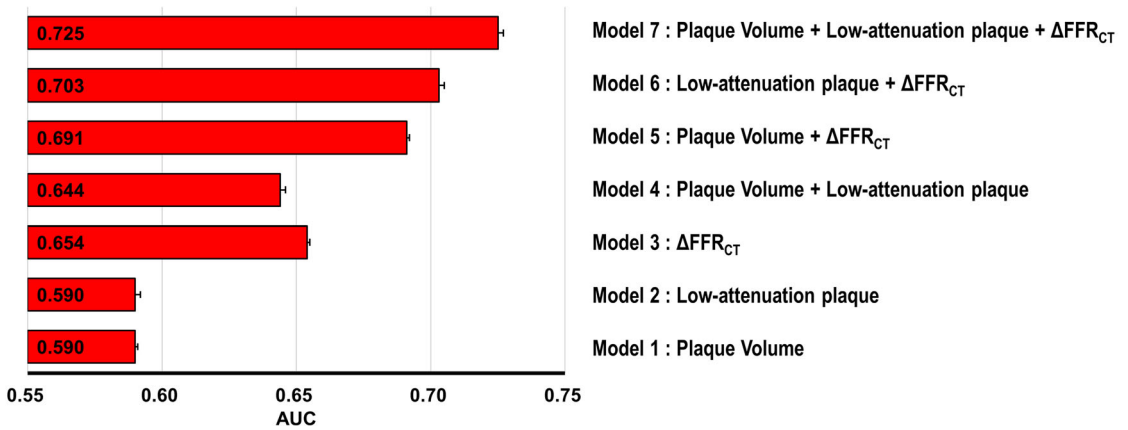

	Model 1	Model 2	Model 3	Model 4	Model 5	Model 6	Model 7
AUC	0.590 (0.589-0.591)	0.590 (0.589-0.592)	0.654 (0.652-0.655)	0.644 (0.643-0.646)	0.691 (0.689-0.692)	0.703 (0.701-0.705)	0.725 (0.724-0.727)
P for difference	Model 1	Model 2	Model 3	Model 4	Model 5	Model 6	Model 7
Model 1	-	0.923	<0.001	<0.001	<0.001	<0.001	<0.001
Model 2		-	<0.001	<0.001	<0.001	<0.001	<0.001
Model 3			-	<0.001	<0.001	<0.001	<0.001
Model 4				-	<0.001	<0.001	<0.001
Model 5					-	<0.001	<0.001
Model 6						-	<0.001

Fig. 4 Performance comparison of various prediction models. Among the prediction models, the model with plaque volume, low-attenuation plaque, and ΔFFR_{CT} showed the highest ability (AUC 0.725, 95% CI 0.724–0.727) in ACS risk prediction. AUC, area under the curve; ΔFFR_{CT}, change in FFR_{CT} across the lesion

Comprehensive integration of anatomical, plaque, and hemodynamic characteristics for detection of high-risk non-obstructive lesions

Despite the vast amount of clinical data, the positive predictive value of each lesion characteristic in the prediction of future cardiovascular events is still low [26, 27]. Our study investigated the prediction ability of individual or combinations of lesion characteristics for ACS risk. Although a prediction model with ΔFFR_{CT} showed the highest performance (AUC 0.654, 95% CI 0.652–0.655) among the individual lesion characteristics, the model comprising ΔFFR_{CT}, low-attenuation plaque, and plaque volume demonstrated the highest predictive ability for ACS risk (AUC 0.725, 95% CI 0.724–0.727). Our results suggest that a comprehensive approach through the integration of information contained in multiple aspects of the coronary lesions can enhance the ability to identify high-risk plaques that can cause ACS in patients with non-obstructive lesions.

Limitations

There are some limitations to our study. First, the number of lesions included in our study was relatively small. Second, as we analyzed per-vessel comparison between culprit and non-culprit lesions from ACS patients, there was no external control for the study. Third, patients with inadequate or poor CCTA image were excluded for analysis [8]. As the current study retrospectively analyzed the CCTA data, we could not control the CT protocol of the participating center. Therefore, to minimize the bias derived from the image quality, high standard for CCTA image quality was applied for final inclusion. However, the presence of selection bias cannot be completely excluded. Fourth, CCTA images were acquired using different systems according to the participating centers. However, the type of CCTA scanner did not show a significant interaction with the study results. When the type of CCTA scanner was included as a covariable, the significance of ΔFFR_{CT} (adjusted HR 2.86, 95% CI 1.19–6.92, $p = 0.019$) or low-attenuation plaque (adjusted HR 3.24, 95% CI 1.41–7.48, $p = 0.006$) was similarly observed, and overall study results were not changed. Last, diverse factors such as systemic blood pressure, vascular spasticity, and endothelial or microvascular dysfunction could be related to plaque rupture in non-obstructive lesions, which were not considered in our study.

Conclusion

In non-obstructive coronary lesions, ΔFFR_{CT} was the most important factor in the prediction of ACS risk. The integration of anatomical, plaque, and hemodynamic characteristics can improve the noninvasive prediction of ACS risk for patients with non-obstructive coronary lesions.

Funding This study was funded by HeartFlow Inc. The company performed the computational fluid dynamics analysis, but had no role in study design, study conduct, or manuscript preparation.

Compliance with ethical standards

Conflict of interest Dr. Choi, and Dr. Taylor are employees of HeartFlow, Inc. Dr. De Bruyne is a shareholder for HeartFlow.

Guarantor The scientific guarantor of this publication is BK Koo.

Statistics and biometry No complex statistical methods were necessary for this paper.

Informed consent Written informed consent was waived by the Institutional Review Board.

Ethical approval The study protocol was approved by the institutional review board. The clinical trial registration number of this article is NCT02374775.

Methodology
- retrospective
- observational study
- multi-center study

References

1. Ferencik M, Mayrhofer T, Bittner DO et al (2018) Use of high-risk coronary atherosclerotic plaque detection for risk stratification of patients with stable chest pain: a secondary analysis of the promise randomized clinical trial. JAMA Cardiol 3:144–152
2. Dey D, Gaur S, Ovrehus KA et al (2018) Integrated prediction of lesion-specific ischaemia from quantitative coronary CT angiography using machine learning: a multicentre study. Eur Radiol 28:2655–2664
3. Coenen A, Lubbers MM, Kurata A et al (2017) Diagnostic value of transmural perfusion ratio derived from dynamic CT-based myocardial perfusion imaging for the detection of haemodynamically relevant coronary artery stenosis. Eur Radiol 27:2309–2316
4. van Hamersvelt RW, Zreik M, Voskuil M, Viergever MA, Isgum I, Leiner T (2019) Deep learning analysis of left ventricular myocardium in CT angiographic intermediate-degree coronary stenosis improves the diagnostic accuracy for identification of functionally significant stenosis. Eur Radiol 29:2350–2359
5. Lee JM, Doh JH, Nam CW, Shin ES, Koo BK (2018) Functional approach for coronary artery disease: filling the gap between evidence and practice. Korean Circ J 48:179–190
6. Kim HJ, Vignon-Clementel IE, Coogan JS, Figueroa CA, Jansen KE, Taylor CA (2010) Patient-specific modeling of blood flow and pressure in human coronary arteries. Ann Biomed Eng 38:3195–3209
7. Min JK, Taylor CA, Achenbach S et al (2015) Noninvasive fractional flow reserve derived from coronary CT angiography: clinical data and scientific principles. JACC Cardiovasc Imaging 8:1209–1222
8. Taylor CA, Fonte TA, Min JK (2013) Computational fluid dynamics applied to cardiac computed tomography for noninvasive

quantification of fractional flow reserve scientific basis. J Am Coll Cardiol 61:2233–2241
9. Siogkas PK, Anagnostopoulos CD, Liga R et al (2019) Noninvasive CT-based hemodynamic assessment of coronary lesions derived from fast computational analysis: a comparison against fractional flow reserve. Eur Radiol 29:2117–2126
10. Lee JM, Choi G, Koo BK et al (2018) Identification of high-risk plaques destined to cause acute coronary syndrome using coronary computed tomographic angiography and computational fluid dynamics. JACC Cardiovasc Imaging. https://doi.org/10.1016/j.jcmg.2018.01.023
11. Katritsis DG, Gersh BJ, Camm AJ (2016) A clinical perspective on sudden cardiac death. Arrhythmia Electrophysiol Rev 5:177–182
12. Myerburg RJ, Junttila MJ (2012) Sudden cardiac death caused by coronary heart disease. Circulation 125:1043–1052
13. Motoyama S, Ito H, Sarai M et al (2015) Plaque characterization by coronary computed tomography angiography and the likelihood of acute coronary events in mid-term follow-up. J Am Coll Cardiol 66:337–346
14. Maurovich-Horvat P, Ferencik M, Voros S, Merkely B, Hoffmann U (2014) Comprehensive plaque assessment by coronary CT angiography. Nat Rev Cardiol 11:390–402
15. Park JB, Choi G, Chun EJ et al (2016) Computational fluid dynamic measures of wall shear stress are related to coronary lesion characteristics. Heart 102:1655–1661
16. Hall MA, Holmes G (2003) Benchmarking attribute selection techniques for discrete class data mining. IEEE Trans Knowl Data Eng 15:1437–1447
17. Bourantas CV, Garcia-Garcia HM, Farooq V et al (2013) Clinical and angiographic characteristics of patients likely to have vulnerable plaques: analysis from the PROSPECT study. JACC Cardiovasc Imaging 6:1263–1272
18. Kristensen TS, Kofoed KF, Kuhl JT, Nielsen WB, Nielsen MB, Kelbaek H (2011) Prognostic implications of nonobstructive coronary plaques in patients with non-ST-segment elevation myocardial infarction: a multidetector computed tomography study. J Am Coll Cardiol 58:502–509
19. Ferraro RA, Lin F, Peña J et al (2018) High-risk plaque in non-obstructive coronary artery disease confers risk similar to obstructive disease without high-risk features: the iconic study. J Am Coll Cardiol 71:A103
20. Samady H, Eshtehardi P, McDaniel MC et al (2011) Coronary artery wall shear stress is associated with progression and transformation of atherosclerotic plaque and arterial remodeling in patients with coronary artery disease. Circulation 124:779–788
21. Lee J, Choi G, Hwang D et al (2017) Impact of longitudinal lesion geometry on location of plaque rupture and clinical presentations. JACC Cardiovasc Imaging 10:677–688
22. Lee JM, Koo BK, Shin ES et al (2017) Clinical outcomes of deferred lesions with angiographically insignificant stenosis but low fractional flow reserve. J Am Heart Assoc 6:e006071
23. Ford TJ, Berry C, De Bruyne B et al (2017) Physiological predictors of acute coronary syndromes: emerging insights from the plaque to the vulnerable patient. JACC Cardiovasc Interv 10:2539–2547
24. Choi G, Lee JM, Kim HJ et al (2015) Coronary artery axial plaque stress and its relationship with lesion geometry: application of computational fluid dynamics to coronary CT angiography. JACC Cardiovasc Imaging 8:1156–1166
25. Gijsen FJ, Wentzel JJ, Thury A et al (2008) Strain distribution over plaques in human coronary arteries relates to shear stress. Am J Physiol Heart Circ Physiol 295:H1608–H1614
26. Kaul S, Narula J (2014) In search of the vulnerable plaque: is there any light at the end of the catheter? J Am Coll Cardiol 64:2519–2524
27. Koskinas KC, Ughi GJ, Windecker S, Tearney GJ, Raber L (2016) Intracoronary imaging of coronary atherosclerosis: validation for diagnosis, prognosis and treatment. Eur Heart J 37:524–535a-c

Affiliations

Jiesuck Park[1] · Joo Myung Lee[2] · Bon-Kwon Koo[1,3] · Gilwoo Choi[4] · Doyeon Hwang[1] · Tae-Min Rhee[1] · Seokhun Yang[1] · Jonghanne Park[1] · Jinlong Zhang[1] · Kyung-Jin Kim[1] · Yaliang Tong[5] · Joon-Hyung Doh[6] · Chang-Wook Nam[7] · Eun-Seok Shin[8] · Young-Seok Cho[9] · Eun Ju Chun[10] · Jin-Ho Choi[2] · Bjarne L. Norgaard[11] · Evald H. Christiansen[11] · Koen Nieman[12,13] · Hiromasa Otake[14] · Martin Penicka[15] · Bernard de Bruyne[15] · Takashi Kubo[16] · Takashi Akasaka[16] · Jagat Narula[17] · Pamela S. Douglas[18] · Charles A. Taylor[4,19]

1 Department of Internal Medicine and Cardiovascular Center, Seoul National University Hospital, 101 Daehang-ro, Chongno-gu, Seoul 110-744, Republic of Korea

2 Department of Internal Medicine and Cardiovascular Center, Heart Vascular Stroke Institute, Samsung Medical Center, Sungkyunkwan University School of Medicine, Seoul, Republic of Korea

3 Institute on Aging, Seoul National University, Seoul, Republic of Korea

4 HeartFlow, Inc., Redwood City, CA, USA

5 Department of Cardiology, China-Japan Union Hospital of Jilin University, Changchun, China

6 Department of Medicine, Inje University Ilsan Paik Hospital, Goyang, Republic of Korea

7 Department of Medicine, Keimyung University Dongsan Medical Center, Daegu, Republic of Korea

8 Department of Cardiology, Ulsan Hospital, Ulsan, Republic of Korea

9 Department of Medicine, Seoul National University Bundang Hospital, Seongnam, Republic of Korea

10 Department of Radiology, Seoul National University Bundang Hospital, Seongnam, Republic of Korea

11 Department of Cardiology, Aarhus University Hospital, Aarhus, Denmark

[12] Erasmus University Medical Center, Rotterdam, Netherlands

[13] Cardiovascular Institute, Stanford University, School of Medicine, Stanford, CA, USA

[14] Department of Internal Medicine, Division of Cardiovascular and Respiratory Medicine, Kobe University Graduate School of Medicine, Kobe, Japan

[15] Cardiovascular Center Aalst, OLV-Clinic, Aalst, Belgium

[16] Department of Cardiovascular Medicine, Wakayama Medical University, Wakayama, Japan

[17] Icahn School of Medicine at Mount Sinai Hospital, New York, NY, USA

[18] Duke Clinical Research Institute, Duke University School of Medicine, Durham, NC, USA

[19] Department of Bioengineering, Stanford University, Stanford, CA, USA